Journal of Membrane Science 660 (2022) 120875

Contents lists available at ScienceDirect

Journal of Membrane Science

journal homepage: www.elsevier.com/locate/memsci

Oxygen permeability and surface kinetics of composite oxygen transport membranes based on stabilized δ-Bi_2O_3

Linn Katinka Emhjellen [a,*], Wen Xing [b], Zuoan Li [b], Reidar Haugsrud [a,**]

[a] Department of Chemistry, Centre for Materials Science and Nanotechnology, University of Oslo, FERMiO, Gaustadalléen 21, NO-0349, Oslo, Norway
[b] SINTEF Industry, Sustainable Energy Technology, Pb. 124 Blindern, NO-0314, Oslo, Norway

ARTICLE INFO

Keywords:
Oxygen transport composite membrane
Oxygen permeability
Surface kinetics

ABSTRACT

Composite ceramic membranes based on the ionic conducting Tm-stabilized δ-Bi_2O_3 (BTM) and the electronic conducting $(La_{0.8}Sr_{0.2})_{0.99}MnO_{3-\delta}$ (LSM) exhibit among the highest oxygen flux values reported for Bi_2O_3-based membranes. Here, we use pulse-response isotope exchange (PIE) and oxygen flux measurements to elaborate on limiting factors for the oxygen permeation in BTM - 40-70 vol% LSM composites. Once both phases percolate, between 30 and 50 vol% BTM, the flux is essentially independent of the BTM/LSM volume ratio. The oxygen permeability is under mixed diffusion- and surface control, gradually becoming more bulk-limited with increasing temperature. The oxygen exchange coefficients of BTM-LSM are significantly higher than its constituent phases, revealing that a cooperative surface exchange mechanism enhances the kinetics. Some of the Tm was substituted with Pr to introduce electronic conductivity in BTM. $(Bi_{0.8}Tm_{0.15}Pr_{0.05})_2O_{3-\delta}$ (BTP) exhibits higher surface exchange coefficients compared to BTM, but the oxygen flux remains one order of magnitude lower than that of percolating BTM-LSM composites.

1. Introduction

Dense, ceramic oxygen transport membranes (OTMs) combining high oxygen flux with chemical and mechanical stability find applications such as in oxy-fuel combustion and reactors for partial oxidation of methane. A few single-phase materials have shown the required transport properties, but suffer from reactivity towards acidic gases [1], while others have high thermal expansion coefficients [2] or detrimental phase transitions in the temperature window of operation, all hampering technological implementation [3]. Oxygen transport in dual-phase membranes is commonly limited by the oxide ion conductivity.

In its narrow stability range from approximately 825 to 730 °C, cubic bismuth oxide (δ-Bi_2O_3) exhibits the highest reported oxide ion conductivity among binary oxides [4,5]. In order to prevent phase transition to the poorly conducting α-phase, the δ-phase is stabilized to lower temperatures by substitution with rare-earth cations of similar radii and the same valence as Bi [6–11]. Since the electronic conductivity of Bi_2O_3 is inherently low, Bi_2O_3-based phases need to be combined with an electronic conductor to reach appreciable oxygen fluxes [12]. There are several reports in the literature on composites between stabilized δ-Bi_2O_3 and a metallic phase (cermet) consisting of either Ag or Au. The highest flux has been achieved with 40 vol% Ag, where the oxygen flux increases by 1–2 orders of magnitude compared to single-phase Bi_2O_3, mainly attributed to improved electronic conductivity [12–15]. Effects of the metallic phase on the surface exchange kinetics are elusive with conflicting literature results [12–14,16–18].

Ceramic mixed conducting composites comprising oxide ion and electronic conducting phases are alternatives to cermets and single-phase mixed oxide ion-electron conductors [19,20]. Oxide ion conductors such as Gd-doped ceria and Y-stabilized zirconia combined with an electronically conducting oxide have been tested as OTMs, yielding only moderate oxygen fluxes [21–26]. We have recently reported a composite membrane of 60 vol% $(Bi_{0.8}Tm_{0.2})_2O_{3-\delta}$ (BTM) and 40 vol% $(La_{0.8}Sr_{0.2})_{0.99}MnO_{3-\delta}$ (LSM) that shows high oxygen fluxes - comparable to that of e.g., $Ba_{0.5}Sr_{0.5}Co_{0.8}Fe_{0.2}O_{3-\delta}$ (BSCF) [27].

The present contribution addresses the surface and bulk properties of the BTM-LSM system to determine the limiting factors for the oxygen permeation. We seek to optimize the performance by improving the microstructure and varying the BTM/LSM volume ratio. To examine the potential of stabilized δ-Bi_2O_3 as a single-phase OTM, we introduce

* Corresponding author.
** Corresponding author.
E-mail addresses: l.k.emhjellen@smn.uio.no (L.K. Emhjellen), reidar.haugsrud@kjemi.uio.no (R. Haugsrud).

https://doi.org/10.1016/j.memsci.2022.120875
Received 14 March 2022; Received in revised form 13 July 2022; Accepted 26 July 2022
Available online 31 July 2022

mixed conductivity in BTM by substituting some of the Tm with Pr, yielding $(Bi_{0.8}Tm_{0.15}Pr_{0.05})_2O_{3-\delta}$ (BTP). Flux measurements were performed as a function of temperature and oxygen partial pressure gradient, and oxygen exchange coefficients were measured as a function of temperature by means of pulse-response isotope exchange (PIE).

2. Experimental

Powders of $(Bi_{0.8}Tm_{0.2})_2O_3$ (BTM) and $(Bi_{0.8}Tm_{0.15}Pr_{0.05})_2O_{3-\delta}$ (BTP) were synthesized by solid-state reactions. $(La_{0.8}Sr_{0.2})_{0.99}MnO_{3-\delta}$ (LSM) powder synthesized by spray pyrolysis was purchased from Cerpotech AS. The BTM-LSM composites were made by mixing defined volume ratios of the constituent phases, pressing pellets and finally sintering at 1000 °C for 10 h. Table 1 presents the compositions investigated in this work. For more details, see S-2.2 in the Supporting Information.

The sintered membranes were sealed to the alumina support tube of a ProboStat™ measurement cell using a gold ring. Mass flow controllers defined the supply of O_2, He and N_2 feed gas mixtures and Ar sweep gas. The composition of the sweep gas was measured at the outlet with a gas chromatograph (GC). Oxygen flux measurements were performed in the temperature range 600–900 °C (S-2.2 for details).

Oxygen exchange kinetics of BTM, BTP, BTM-LSM 60/40, BTM-LSM 50/50 and BTM-LSM 30/70 were investigated by means of PIE [28]. Powders of 90–125 μm dense particles were studied in the temperature range 600–900 °C at a p_{O_2} of 0.21 atm. $A^{16}O_2/N_2$ (21% $^{16}O_2$ in N_2) gas mixture with a flow rate of 50 ml/min (STP) was used as carrier gas. The $^{18}O_2$/Ar (21% $^{18}O_2$ in Ar) pulse response was analyzed at the exit of the reactor using a quadrupole mass spectrometer (MS) (S-2.3 for details).

3. Results

Fig. 1 presents the temperature dependence of the oxygen flux for single-phase BTP and samples with different volume ratios of BTM and LSM. The oxygen flux of BTM-LSM 30/70 is more than one order of magnitude lower than for the 50/50 and 60/40 compositions, reflecting that more than 30 vol% of BTM is required to form a percolating BTM network in the composite. This is in line with the SEM micrographs of cross-sections displayed in Fig. 2. The oxygen flux of BTP is higher than the 30/70 composition, but still approximately one order of magnitude lower than for the compositions with percolating phases. For all BTM-LSM composites, the temperature dependence of the oxygen flux deviates from Arrhenius behavior; the apparent activation energy decreases with increasing temperature from 130 to 65 kJ/mol. Note that each temperature has slightly varying oxygen chemical potential gradient.

Fig. 3 presents the oxygen flux as a function of the chemical potential gradient for BTM-LSM 50/50 every 50 °C from 600 to 900 °C. Clearly, there are discrepancies from a linear behavior, and extrapolation back to zero gradient, consequently, deviates from origin. The same behavior was reported for the BTM-LSM 60/40 in Ref. [27]. As outlined further in S-1, dedicated analyses are often required to conclude upon the rate limiting processes based on functional oxygen pressure dependences.

Table 1
Sample abbreviations, phase compositions and volumetric ratios for the samples in this work.

Sample abbreviations	Phase A	Phase B	Volumetric ratio, A and B
BTM	$(Bi_{0.8}Tm_{0.2})_2O_3$	–	100 %
BTM-LSM 30/70	$(Bi_{0.8}Tm_{0.2})_2O_3$	$(La_{0.8}Sr_{0.2})_{0.99}MnO_{3-\delta}$	30 % and 70 %
BTM-LSM 50/50	$(Bi_{0.8}Tm_{0.2})_2O_3$	$(La_{0.8}Sr_{0.2})_{0.99}MnO_{3-\delta}$	50 % and 50 %
BTM-LSM 60/40	$(Bi_{0.8}Tm_{0.2})_2O_3$	$(La_{0.8}Sr_{0.2})_{0.99}MnO_{3-\delta}$	60 % and 40 %
BTP	$(Bi_{0.8}Tm_{0.15}Pr_{0.05})_2O_{3-\delta}$	–	100 %

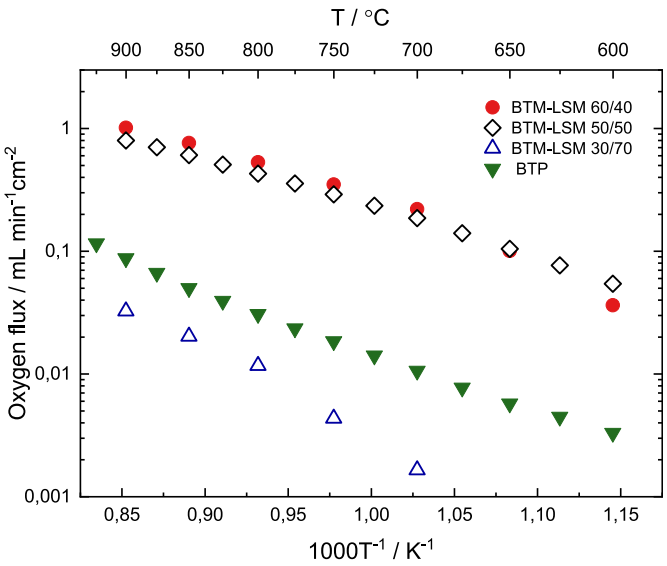

Fig. 1. Oxygen flux as a function of inverse temperature for BTM-LSM composite membranes with different phase ratios. The data for BTM-LSM 60/40 is taken from Ref. [27]. The thickness of BTM-LSM 60/40 is 1.35 mm, while both BTM-LSM 50/50 and BTM-LSM 30/70 are 1.5 mm thick. The thickness of BTP is 1.3 mm.

The nonlinear behaviors in Fig. 1 indicate that more than one process affects the overall oxygen permeation. The transport properties of BTM and LSM render high ambipolar oxide ion-electron conductivity which may result in effects of surface kinetics on the oxygen permeation, even for millimeter thick membranes. Aiming to further rationalize the data, the oxygen exchange kinetics was investigated. Fig. 4 shows an Arrhenius representation of the oxygen exchange coefficient, *k*, for BTP, BTM, BTM-LSM 60/40, 50/50 and 30/70 composites and, moreover, literature data for LSM [29]. The composites exhibit significantly higher oxygen exchange coefficients than their constituent phases; one order of magnitude higher than BTM and two orders of magnitude higher than LSM. The volume ratio of BTM and LSM has only a minor influence on the value and temperature dependence of *k*. BTP exhibits higher oxygen exchange coefficients than the other two single-phase materials.

Disregarding that *k* does not strictly follow Arrhenius behavior, the BTM-LSM composites exhibit apparent activation energies for oxygen exchange in the same range as single-phase BTM and LSM [29], varying between 110 and 140 kJ/mol.

4. Discussion

To rationalize the oxygen flux characteristics, we use the temperature and oxygen pressure dependence of the flux data and the surface kinetics measurements in combination with literature data on the electrical conductivity [10]. We address three different limiting cases; pure diffusion control, and surface kinetics control with linear and non-linear relations between the oxygen chemical potential gradient and the oxygen flux. Details on the models, the assumptions and data analyses are presented in the Supporting Information, S-1 to S-3.

The relation between the flux and the oxygen chemical potential gradient is linear for surface-controlled oxygen flux as long as the gradient across the permeate side is relatively small. For large p_{O_2} gradients, however, nonlinear relations are prone to affect interpretation of oxygen flux data. As for the present dataset, we have applied a Butler-Volmer based formalism to assess effects of large chemical potential gradients across the permeate side solid-gas interface (S-3.1 and S-3.2, Fig. S-2 a and b) [30–32]. Moreover, the oxygen flux assuming bulk control was estimated using literature data on the electrical conductivity

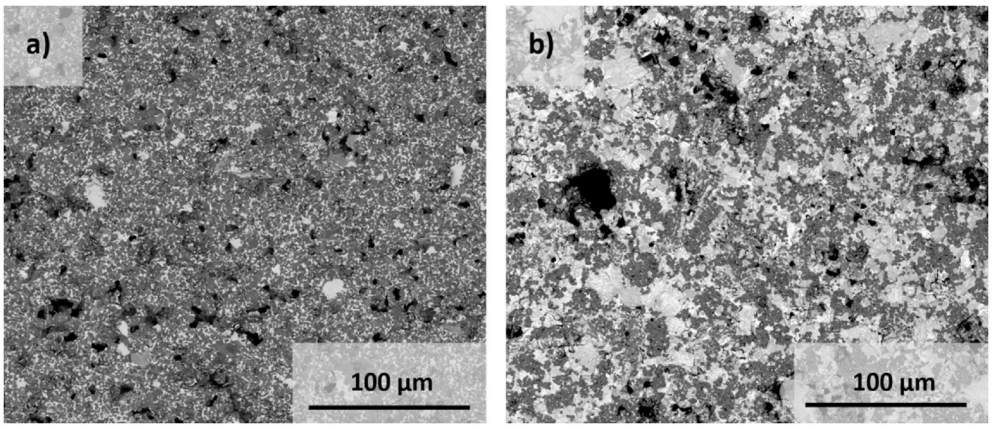

Fig. 2. Cross-sections of BTM-LSM membranes with BTM/LSM volume ratios of a) 30/70 and b) 60/40 in a BSE SEM micrograph. The bright and dark areas are BTM and LSM, respectively.

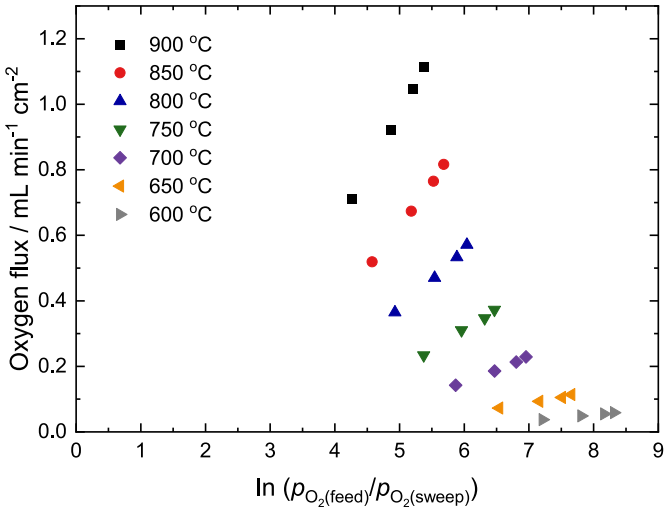

Fig. 3. Oxygen flux of BTM-LSM 50/50 plotted as a function of oxygen partial pressure gradient. The p_{O_2} in the feed was varied from 0.2 to 1 atm and the p_{O_2} in the permeate was measured by the GC.

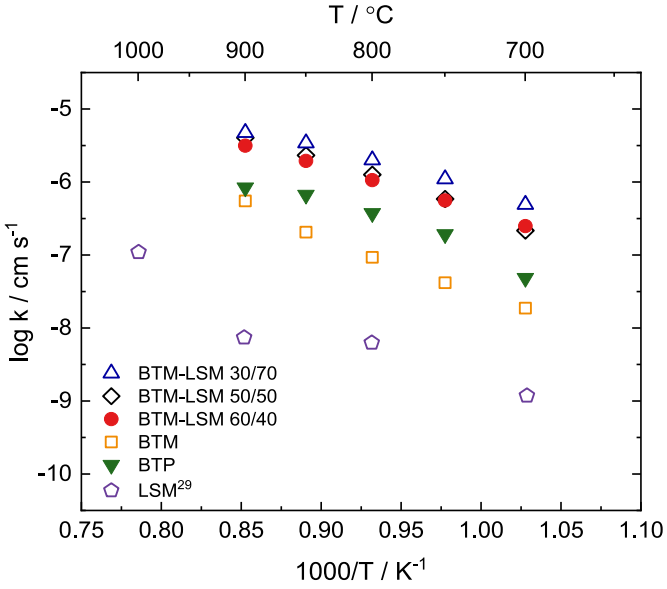

Fig. 4. Oxygen exchange coefficient for BTP, BTM and BTM-LSM composite membranes of different ratios as a function of inverse temperature at 0.21 atm O_2. Also shown are data for LSM, obtained by ^{18}O–^{16}O isotope exchange followed by depth profiling in ~ 1 atm O_2 [29].

of BTM. Fig. 5 shows that the BTM-LSM 60/40 flux data fall between the estimated surface- and diffusion controlled flux. The oxygen flux increases due to the large interfacial chemical potential gradient when surface kinetics is limiting (see also Fig. S-2). With increasing temperature, both the measured flux values and the apparent activation energy gradually approach the estimated diffusion-controlled flux. One should recognize that the effect of the nonlinear relation between the flux and the potential gradient depends on the parameter β (see S-3).

The relative influence of surface and bulk processes on the overall oxygen flux can be expressed by the ratio between the surface exchange kinetics and the ambipolar diffusion. Here we will adhere to the Biot number, as defined in S-Eq.12 [33–35] (S-3.4, Fig. S-4) and presented in Fig. 6 for the BTM-LSM 60/40 membrane. The Biot number increases with increasing temperature, but the values remain essentially within the range representing mixed rate control [32]. One should recognize that the Biot numbers determined using the measured surface kinetics data (cf. Fig. 4) are lower than those estimated from modelling of the flux data.

Alternatively, following the procedure by Chen et al. [14], flux data and ambipolar conductivity can be applied to derive resistances in series for surface and bulk kinetics in a simplified equivalent circuit. The resistances of the two processes are equal at approximately 830 °C (cf. Fig S-1, S-3.1 for derivation). Above this temperature, the resistance related to ambipolar conductivity is higher than that for oxygen exchange. This is in reasonably good agreement with the Biot numbers in Fig. 6.

As encountered in Fig. 3, the oxygen pressure dependence on the oxygen flux was not directly proportional to the chemical potential gradient. Analyses in S-3.3 (Fig. S-4) show that the oxygen flux is rather close to being proportional to $(p_{O_2}^{1/4}(I) - p_{O_2}^{1/4}(II))$. Ten Elsof et al. [12] reported virtually the same characteristics for a BE25-40Ag cermet - both the actual values of the oxygen flux and their functional dependences on the measurement conditions.

The significant increase in the oxygen flux for Bi_2O_3 based materials with addition of an electronic conductor could principally originate only from the high electronic conductivity of the second phase. However, there is potentially an additional gain from enhancement of the surface exchange kinetics. This is encountered by the increase in the oxygen flux with the more catalytically active Ag compared with Au as the metallic phase of BE25 based cermets [14]. Although single-phase Bi_2O_3 based materials have shown remarkably high oxygen surface exchange, far better than for LSM [11,29,36], the superior oxygen fluxes of BTM-LSM show that LSM contributes more than by promoting the electronic

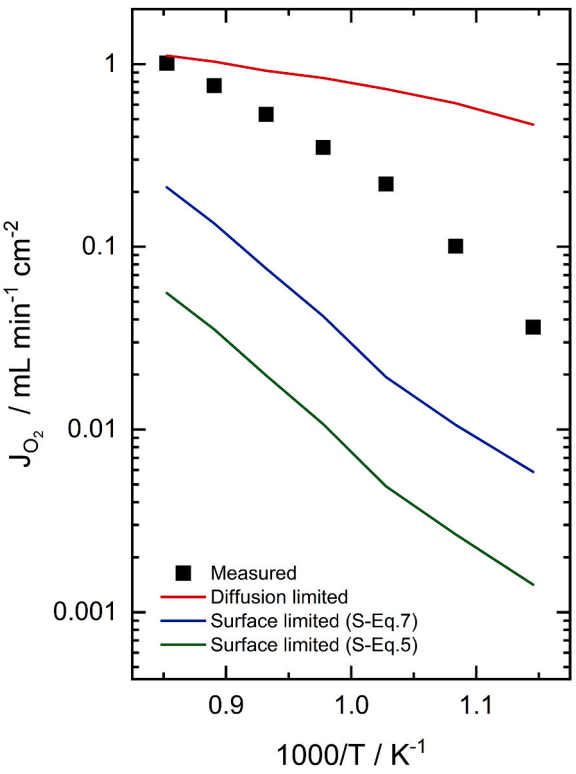

Fig. 5. Measured and estimated oxygen flux as a function of inverse temperature for BTM-LSM 60/40. The diffusion limited flux is derived from literature ambipolar conductivities (S-Eq. 4). The fluxes under surface limitation are derived based on the surface exchange coefficients in Fig. 4 for linear (S-Eq. 5) and nonlinear (S-Eq. 7) relations to the oxygen chemical potentials, with $\beta = 0.35$. In all three cases it is assumed that the entire oxygen potential gradient is across the respective region, i.e., bulk and permeate side solid-gas interface.

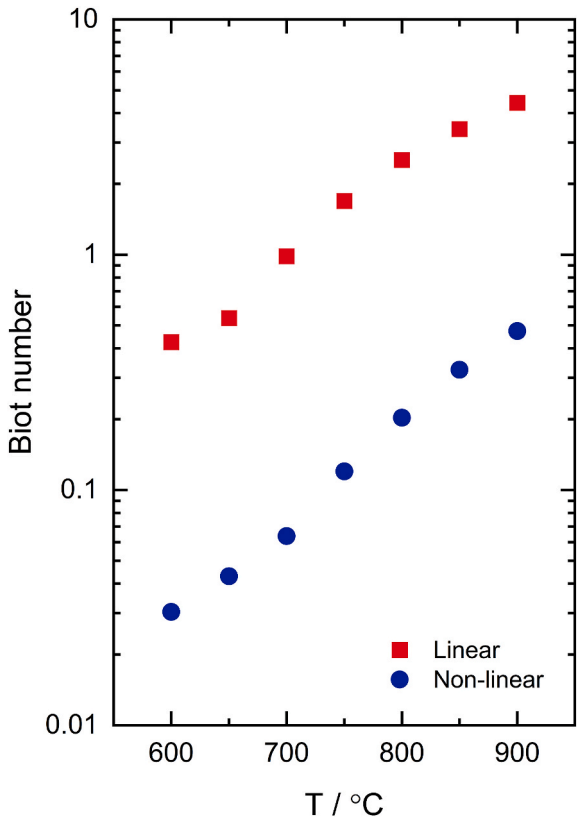

Fig. 6. Temperature dependence of the Biot number (S-Eq. 12) based on different analyses (S-3.4, Fig. S-4) of the oxygen flux data for BTM-LSM 60/40 (Fig. 1), surface kinetics data (Fig. 4), and literature values for the ambipolar oxide ion electron transport.

conductivity. This is in line with the significant increase in the oxygen surface exchange coefficient when merging LSM with BTM (cf. Fig. 4), unarguably showing that LSM plays a role in the surface exchange mechanism of the composites. Based on the relatively low concentration of electron holes in Bi_2O_3, one may speculate whether spill-over of electronic species from LSM and subsequent surface diffusion of electron holes and O^- on the BTM surface rationalize the enhancement with addition of LSM. This mechanism even accounts for the observed dependence of the oxygen pressure gradient and is in correspondence with the hypothesis of ten Elsof et al. [12].

There are controversial reports in the literature as to whether triple-phase-boundaries (TPBs) contribute or not to the generally higher oxygen fluxes for composites compared to single-phase materials [35, 48] [47]. Since the phases in the BTM-LSM composites are not that well dispersed, optimization of the fabrication giving less agglomeration should yield better oxygen flux performance if the TPB is important to the surface kinetic. However, as evident from S-5 we did not come to any conclusive results.

Concentration polarization (gas-phase double-layers) may affect oxygen flux measurements, particularly for materials with high oxygen fluxes. Evaluation of the present dataset, however, reveals only a minor effect (S-3.5, Fig. S-5). This is in line with the hypothesis of surface diffusion controlled oxygen exchange kinetics, since double layers are expected to be less prominent for mechanisms with surface diffusion as the *rds*. In this respect, it should be recognized that, analyses based on the Butler-Volmer relations become less adequate if surface diffusion represents the *rds*. However, surface diffusion of charged species across space charge layers at the composite phase boundaries may introduce potential differences introducing polarization that has been described by Butler-Volmer type formalisms [37].

The above assessments establish that the oxygen flux data are in the mixed regime, essentially surface controlled below 750 °C, gradually approaching bulk control at the highest temperatures. Still the analyses are based on limiting situations where the crux of the matter is the distribution of the oxygen chemical potential and how it changes with temperature. Dissimilar oxygen gradients require different approaches to analyze the data and may therefore give rise to divergent conclusions. Most importantly is the implementation of non-linear relations between the oxygen flux and the oxygen chemical potential as a consequence of the precipitous gradient assumed at the permeate side solid-gas interface. However, the oxygen exchange coefficients derived from the linear and non-linear relation do not differ enough to change the main conclusion.

Finally, we compare the oxygen flux of BTM-LSM and BTP with the relevant literature. Fig. 7 shows the oxygen flux of BTM-LSM 60/40 and BTP together with several single- and dual-phase membranes based on Bi_2O_3 [12–14]. The BTM-LSM 60/40 composite exhibits among the highest oxygen flux values of all reported Bi_2O_3-based membranes so far. The oxygen permeation of BE25 is presumably limited by the minute *p*-type conductivity restricting both surface and bulk processes [15,36]. The increased oxygen flux of 1–2 orders of magnitude of BE25-Ag40 compared to that of BE25 is mainly due to the enhanced electronic conductivity, although it has been shown that the surface kinetics also improves with Ag additions [12,15]. The reported critical thicknesses of BE25-Ag40 membranes obtained from IEDP-SIMS in 0.2 atm O_2 and oxygen permeation measurements in an air/He gradient were approximately 0.6 and 1 mm at 600 °C and 850 °C, respectively [15,38]. This shows that the 0.13 mm thick BE25-Ag40 membrane [13] is in the surface-limited regime. In contrast to the surface-limited BE25-Ag40 membrane [13], BTM-LSM 60/40 has the potential to reach even higher flux values by reducing the membrane thickness.

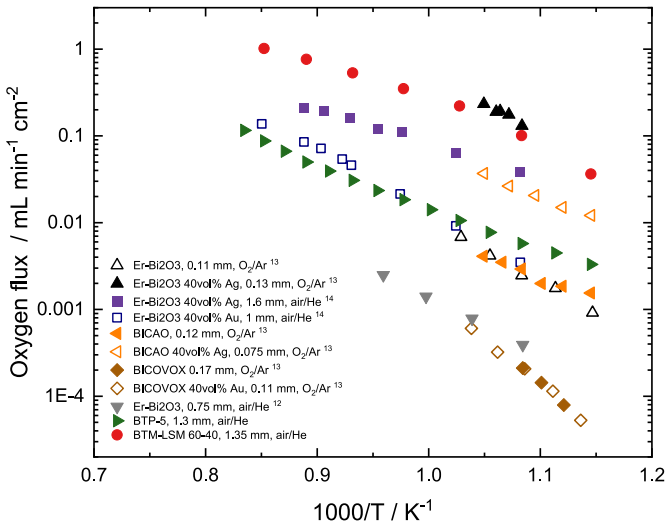

Fig. 7. Oxygen flux of single- and dual-phase Bi_2O_3-based OTMs as a function of temperature [12–14]. Note that the values are not directly comparable due to the difference in thickness, but also due to the varying chemical potential gradients among the different datasets.

$(Bi_2O_3)_{0.75}(CaO)_{0.27}$ (BICAO) membranes show the same behavior as BE25. However, the addition of 40 vol % Au to $Bi_{2.02}Co_{0.13}V_{0.85}O_x$ (BICOVOX) does not affect the oxygen permeation, implying that the flux of BICOVOX is purely limited by surface kinetics. Au is recognized for its poor catalytic activity towards the oxygen reduction reaction, which is also encountered comparing the relative effects of Au and Ag on the oxygen flux for BE25-Au40 and BE25-Ag40 [14].

The oxygen flux of BTP is one order of magnitude higher than for the 0.75 mm thick BE25 membrane reported by ten Elshof et al. [12]. The oxygen permeation of BTP is surface-controlled (cf. Fig. 5b), and it is therefore difficult to ascertain whether the increased electronic conduction also affects the diffusion, and to estimate the effect of the Pr-concentration on the oxygen permeation. However, BTP has potential as a single-phase MIEC membrane, and further studies with higher dopant concentrations could be interesting.

5. Conclusion

Oxygen permeability of BTM-LSM is under mixed diffusion- and surface control, becoming more diffusion-limited with increasing temperature. Above the percolation threshold (between 30 and 50 vol % BTM), the flux increases significantly and is essentially independent of the BTM/LSM volume ratio. The composites exhibit significantly higher oxygen exchange coefficients compared to their constituent phases; one order of magnitude higher than BTM and two orders of magnitude higher than LSM. The BTM/LSM volume ratio has a minor effect on the surface exchange rate. It was speculated whether spill-over of electronic species from LSM and subsequent surface diffusion of electron holes and O^- on the BTM surface may rationalize the overall increase in the oxygen exchange kinetics and the dependence of the oxygen pressure gradient on the permeability. Pr increases the oxygen permeability by partly substituting Tm in BTP due to an increased concentration of electron holes, but the oxygen flux is still one order of magnitude lower than that of BTM-LSM composites with percolating phases.

Credit author statements

Linn Katinka Emhjellen: Writing – Original Draft, Investigation, Visualization.

Wen Xing: Writing – Original Draft, Investigation.

Zuoan Li: Project administration, Writing – Reviewing and Editing.

Reidar Haugsrud: Writing – Reviewing and Editing, Supervision.

Declaration of competing interest

The authors declare that they have no known competing financial interests or personal relationships that could have appeared to influence the work reported in this paper.

Data availability

Data will be made available on request.

Acknowledgments

This work was supported by the Research Council of Norway (RCN) under the CLIMIT program (MOC-OTM 268450). The authors are grateful to Dr. Vincent Thoréton (RCN Fripro project FUSKE 262393) for development and discussions on the gas-phase methodologies.

Appendix A. Supplementary data

Supplementary data to this article can be found online at https://doi.org/10.1016/j.memsci.2022.120875.

References

[1] X. Zhu, et al., Operation of perovskite membrane under vacuum and elevated pressures for high-purity oxygen production, J. Membr. Sci. 345 (1) (2009) 47–52.
[2] R. Kriegel, R. Kircheisen, J. Töpfer, *Oxygen stoichiometry and expansion behavior of $Ba_{0.5}Sr_{0.5}Co_{0.8}Fe_{0.2}O_{3-\delta}$*, Solid State Ionics 181 (1) (2010) 64–70.
[3] Z. Yáng, et al., *Oxygen-vacancy-related structural phase transition of $Ba_{0.8}Sr_{0.2}Co_{0.8}Fe_{0.2}O_{3-\delta}$*, Chem. Mater. 23 (13) (2011) 3169–3175.
[4] M. Yashima, D. Ishimura, *Crystal structure and disorder of the fast oxide-ion conductor cubic Bi_2O_3*, Chem. Phys. Lett. 378 (3) (2003) 395–399.
[5] N.M. Sammes, et al., Bismuth based oxide electrolytes— structure and ionic conductivity, J. Eur. Ceram. Soc. 19 (10) (1999) 1801–1826.
[6] R. Punn, et al., *Enhanced oxide ion conductivity in stabilized δ-Bi_2O_3*, J. Am. Chem. Soc. 128 (48) (2006) 15386–15387.
[7] P. Shuk, et al., *Oxide ion conducting solid electrolytes based on Bi_2O_3*, Solid State Ionics 89 (3) (1996) 179–196.
[8] H. Iwahara, et al., *Formation of high oxide ion conductive phases in the sintered oxides of the system Bi_2O_3-Ln_2O_3 (Ln = La-Yb)*, J. Solid State Chem. 39 (2) (1981) 173–180.
[9] P.D. Battle, C.R.A. Catlow, L.M. Moroney, *Structural and dynamical studies of δ-Bi_2O_3 oxide-ion conductors: II. A structural comparison of $(Bi_2O_3)_{1-x}(M_2O_3)_x$ for M = Y, Er, and Yb*, J. Solid State Chem. 67 (1) (1987) 42–50.
[10] A. Dapčević, et al., *A new electrolyte based on Tm^{3+}-doped δ-Bi_2O_3-type phase with enhanced conductivity*, Solid State Ionics 280 (2015) 18–23.
[11] C.-Y. Yoo, B.A. Boukamp, H.J.M. Bouwmeester, Oxygen surface exchange kinetics of erbia-stabilized bismuth oxide, J. Solid State Electrochem. 15 (2) (2011) 231–236.
[12] J.E. ten Elshof, et al., *Oxygen Permeation Properties of Dense $Bi_{1.5}Er_{0.5}O_3$-Ag Cermet Membranes*, 2004.
[13] E. Capoen, et al., Oxygen permeation in bismuth-based materials. Part I: sintering and oxygen permeation fluxes, Solid State Ionics 177 (5) (2006) 483–488.
[14] C.S. Chen, A.J. Burggraaf, Stabilized bismuth oxide–noble metal mixed conducting composites as high temperature oxygen separation membranes, J. Appl. Electrochem. 29 (3) (1999) 355–360.
[15] E. Capoen, et al., Oxygen permeation in bismuth-based materials. Part II: characterisation of oxygen transfer in bismuth erbium oxide and bismuth calcium oxide ceramic, Solid State Ionics 177 (5) (2006) 489–492.
[16] M.J. Verkerk, M.W.J. Hammink, A.J. Burggraaf, *Oxygen transfer on substituted ZrO_2, Bi_2O_3, and CeO_2 electrolytes with platinum electrodes: I . Electrode resistance by D-C polarization*, J. Electrochem. Soc. 130 (1) (1983) 70–78.
[17] B.A. Boukamp, et al., The oxygen transfer process on solid oxide/noble metal electrodes, studied with impedance spectroscopy, dc polarization and isotope exchange, Electrochim. Acta 38 (14) (1993) 1817–1825.
[18] B.C.H. Steele, et al., Oxygen surface exchange and diffusion in fast ionic conductors, Solid State Ionics 18–19 (1986) 1038–1044.
[19] H.J.M. Bouwmeester, A.J. Burggraaf, Chapter 10 Dense ceramic membranes for oxygen separation, in: A.J. Burggraaf, L. Cot (Eds.), Membrane Science and Technology, Elsevier, 1996, pp. 435–528.
[20] V.V. Kharton, et al., Perovskite-type oxides for high-temperature oxygen separation membranes, J. Membr. Sci. 163 (2) (1999) 307–317.
[21] V.V. Kharton, et al., *Oxygen transport in $Ce_{0.8}Gd_{0.2}O_{2-\delta}$-based composite membranes*, Solid State Ionics 160 (3) (2003) 247–258.
[22] A.J. Samson, M. Søgaard, P. Vang Hendriksen, *(Ce,Gd)$O_{2-\delta}$-based dual phase membranes for oxygen separation*, J. Membr. Sci. 470 (2014) 178–188.

[23] X. Zhu, W. Yang, Composite membrane based on ionic conductor and mixed conductor for oxygen permeation, AIChE J. 54 (3) (2008) 665–672.
[24] T. Chen, et al., *Synthesis and oxygen permeation properties of a $Ce_{0.8}Sm_{0.2}O_{2-\delta}$–$LaBaCo_2O_{5+\delta}$ dual-phase composite membrane*, J. Membr. Sci. 370 (1) (2011) 158–165.
[25] Y. Lin, et al., Enhancing grain boundary ionic conductivity in mixed ionic–electronic conductors, Nat. Commun. 6 (1) (2015) 6824.
[26] S. Cheng, et al., *A novel CO_2- and SO_2-tolerant dual phase composite membrane for oxygen separation*, Chem. Commun. 51 (33) (2015) 7140–7143.
[27] W. Xing, et al., *Thermochemically stable ceramic composite membranes based on Bi_2O_3 for oxygen separation with high permeability*, Chem. Commun. 55 (24) (2019) 3493–3496.
[28] H.J.M. Bouwmeester, et al., A novel pulse isotopic exchange technique for rapid determination of the oxygen surface exchange rate of oxide ion conductors, Phys. Chem. Chem. Phys. 11 (42) (2009) 9640–9643.
[29] R.A. De Souza, J.A. Kilner, J.F. Walker, *A SIMS study of oxygen tracer diffusion and surface exchange in $La_{0.8}Sr_{0.2}MnO_{3+\delta}$*, Mater. Lett. 43 (1) (2000) 43–52.
[30] S. Kim, et al., Oxygen surface exchange in mixed ionic electronic conductor membranes, Solid State Ionics 121 (1) (1999) 31–36.
[31] P.M. Geffroy, et al., Influence of oxygen partial pressure on the oxygen diffusion and surface exchange coefficients in mixed conductors, J. Eur. Ceram. Soc. 39 (1) (2019) 59–65.
[32] S.B. Adler, X.Y. Chen, J.R. Wilson, Mechanisms and rate laws for oxygen exchange on mixed-conducting oxide surfaces, J. Catal. 245 (1) (2007) 91–109.
[33] J. Song, D. Ning, H.J.M. Bouwmeester, *Influence of alkaline-earth metal substitution on structure, electrical conductivity and oxygen transport properties of perovskite-type oxides $La_{0.6}A_{0.4}FeO_{3-\delta}$ (A = Ca, Sr and Ba)*, Phys. Chem. Chem. Phys. 22 (21) (2020) 11984–11995.
[34] B.A. van Hassel, J.E. ten Elshof, H.J.M. Bouwmeester, *Oxygen permeation flux through $La_{1-y}Sr_yFeO_3$ limited by carbon monoxide oxidation rate*, Appl. Catal. Gen. 119 (2) (1994) 279–291.
[35] M.W. den Otter, et al., Reactor flush time correction in relaxation experiments, J. Electrochem. Soc. 148 (2) (2001) J1.
[36] H.J.M. Bouwmeester, et al., Oxygen semipermeability of erbia-stabilized bismuth oxide, Solid State Ionics 53–56 (1992) 460–468.
[37] D.J. Young, M.J. Dignam, Metal oxidation—II. Kinetics in the thin and very thin film regions under conditions of electron equilibrium, J. Phys. Chem. Solid. 34 (7) (1973) 1235–1250.
[38] C.S. Chen, et al., Thickness dependence of oxygen permeation through erbia-stabilized bismuth oxide-silver composites, Solid State Ionics 99 (3) (1997) 215–219.